UNIVERSITY OF BIRMINGHAM

University of Birmingham
Research at Birmingham

Does deamidation of islet amyloid polypeptide accelerate amyloid fibril formation?

Lam, Yuko P. Y.; Wootton, Christopher A.; Hands-portman, Ian J.; Wei, Juan; Chiu, Cookson K. C.; Romero-Canelón, Isolda; Lermyte, Frederik; Barrow, Mark P.; O'connor, Peter B.

Document Version
Peer reviewed version

Link to publication on Research at Birmingham portal

Does Deamidation of Islet Amyloid Polypeptide Accelerate Amyloid Fibril
Formation?

Yuko P. Y. Lam,[a] Christopher A. Wootton,[a] Ian Hands-Portman,[b] Juan Wei,[a] Cookson
K. C. Chiu,[a] I. Romero-Canelon,[ac] Frederik Lermyte,[a] Mark P. Barrow,[a] Peter B.
O'Connor*[a]

Abstract

Mass spectrometry has been applied to determine the deamidation sites and the
aggregation region of the deamidated human islet amyloid polypeptide (hIAPP).
Mutant hIAPP with iso-aspartic residue mutations at possible deamidation sites
showed very different fibril formation behavior, which correlates with the observed
deamidation-induced acceleration of hIAPP aggregation.

Deamidation is a non-enzymatic post-translational modification (PTM) which
contributes to protein ageing.[1] Deamidation occurs spontaneously in solution at
asparagine (Asn) and glutamine (Gln) residues, and results in formation of
iso-aspartic acid/aspartic acid and γ-glutamic acid/glutamic acid (and their
stereoisomers), respectively.[2, 3] The deamidation rate of Asn is faster than Gln due to
the shorter distance between the main chain amido group (-NH-) and the side chain
amide group ($-NH_2-$).[4, 5] With an additional methylene group ($-CH_2-$) into the
backbone of iso-aspartic acid and γ-glutamic acid; the tertiary structure, stability,
folding, and function of proteins can be dramatically altered by deamidation.[6, 7]
Previous studies showed that deamidation can accelerate fibril formation in certain
cases, including mutated amyloid-β (D7N and D23N) observed in Alzheimer's
disease.[8, 9] Aggregation of β_2-microglobulin from dialysis-associated amyloidosis
disease,[10, 11] and αB-crystallin from human eye lens have also been shown to be
affected by deamidation.[12, 13]

Human islet amyloid polypeptide (hIAPP; also referred to as amylin) is a
37-residue hormone peptide co-secreted with insulin and involved in regulating blood
glucose levels.[14] The concentration of hIAPP is around 1-2% relative to the level of
insulin in secretory granules.[15] hIAPP contains an intramolecular disulfide bond
between Cys-2 and Cys-7, as well as an amidated C-terminus,[16] and is an intrinsically
disordered protein with a low level of persistent helical structure between residues
Asn-3 and Leu-27 in solution.[17] hIAPP is an amyloid protein which contains six Asn
and one Gln as potential deamidation sites. A previous study from Nilsson *et al.*
used a variant of hIAPP segment, residues 20-29 (SNNFPAILSS) which is

non-amyloidogenic and showed that addition of less than 5% of deamidated monomer could accelerate the amyloid fibril formation.[18]   Results from Dunkelberger *et al.* also showed that deamidation of hIAPP disrupted the β-sheet structure around Leu-27, resulting in a morphology change of hIAPP fibrils, along with accelerated fibril formation.[19]   The formation of hIAPP fibrils does not contribute to type II diabetes (T2D); however early oligomers of hIAPP lead to the decline of pancreatic β-cell mass and the failure of islet cell transplantation for T2D treatment.[20-22]   Thus, accelerating the formation of the early oligomers of hIAPP may reduce the graft survival rate.[17, 23]   Deamidation has a significant impact on hIAPP fibril formation,[24, 25] the effects on the deamidation rate, the deamidation site(s), and the effects of isomeric deamidation products of hIAPP, however, have not yet been fully addressed.

MS is a powerful tool for examining deamidation in proteins as the deamidation reaction produces products with a mass shift of +0.984 Da (-NH_2 to -OH) at the deamidated residue, which is readily detected by MS.[26-28]   Previous studies also suggested that deamidation can be directly quantified by measuring the peak area of the non-deamidated and deamidated peaks, thus the percentage of deamidation in the sample can be estimated.[29, 30]   Tandem MS/MS can further locate the deamidation site in proteins, and differentiate the isomeric deamidation products.[2, 26-30] Collisionally activated dissociation (CAD) MS/MS can localise deamidation site via a mass shift (+0.984 Da) appears in b and y ion fragments containing the deamidated residue, while unmodified fragments are observed in the regions not containing deamidated residues.[30]   Electron capture dissociation (ECD) MS/MS can be used to not only localises the deamidation site in protein, but also uses to differentiate the isomeric products of deamidation by the mass shift of +58 and -57 Da at the c and z ion fragments of iso-/γ- deamidation products respectively.   The peak intensity of iso-/γ- deamidation products can also compare with the peak intensity of aspartic acid/glutamic acid in order to determine the ratio of the isomeric products.[29]

In order to localise the deamidation site(s) in the incubated hIAPP solution, CAD MS/MS with a 12 Tesla (T) Fourier transform ion cyclotron mass spectrometer (FTICR MS) was applied.   The y_5 fragment clearly showed a deamidated peak in the incubated sample (Fig. 1B), indicating deamidation occurs at Asn-35 residue in hIAPP. For the b fragments, no deamidated peaks were observed for the first 20 amino acid residues (Fig. 1C); however, a deamidated peak was present corresponding to the b_{21} fragment (Fig. 1D), suggesting deamidation only occurs at Asn-21 but not at Asn-3, Gln-10, and Asn-14 residues.   Furthermore, another deamidated peak was detected corresponding to the b_{22} fragment ion in the incubated solution (Fig. 1E), indicating Asn-22 also deamidates within four weeks at 37°C.
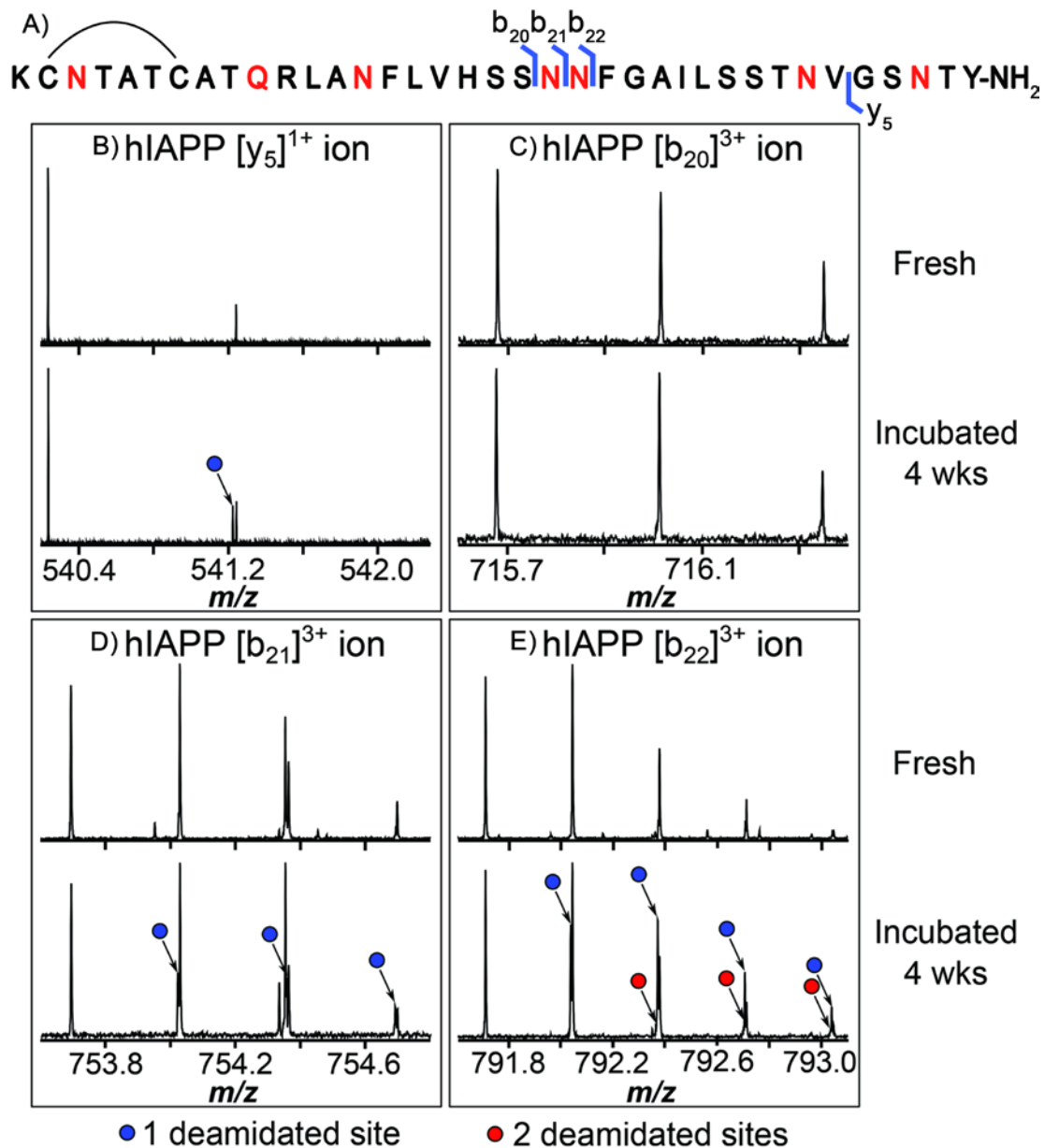
Figure 1. (A) The amino acid sequence of hIAPP. The potential deamidation sites are coloured in red. Key CAD MS/MS fragments of hIAPP revealing deamidation at amino acid residues after 4 weeks incubation at 37°C are shown (B) y_5, (C) b_{20}, (D) b_{21}, and (E) b_{22}. The blue/red circles indicate the isotopic peaks of singly/doubly deamidated fragments, respectively.

Subsequently, MS was applied to determine the deamidation rates of each individual deamidated site in the incubated solutions and resulting fibrils by calculating the percentage ratio between the non-deamidated and the deamidated fragment ion peak areas for each sample. In the incubated solution, the earliest deamidation instance was observed on day 5, and was identified within the y_5 fragment ion (Fig. 2A), indicating the Asn-35 is the first amino acid residue in hIAPP to undergo deamidation, which requires 5-day of incubation at 37°C. Deamidation at

the b_{21} and b_{22} fragment ions was observed on day 8, suggesting Asn-21 and Asn-22 residues are the next amino acid residue to deamidate in hIAPP and require a longer incubation time for deamidation compared to Asn-35 residue. Though the extent of deamidation increased with the incubation time; a similar percentage and rate of deamidation were found in the y_5, b_{21}, and b_{22} fragment ions at the various time points for the incubated solutions. After 28 days incubation, each deamidated fragment ion (y_5, b_{21}, and b_{22}) of the soluble hIAPP showed ~18% deamidation, indicating even though the initial deamidation time between Asn-21, Asn-22, and Asn-35 residues are different, the extent as well as the rate of deamidation of these residues are similar across and at the end of the incubation time. The insoluble protein pellets formed over the course of the incubation were re-solubilised and showed a greater extent of deamidation than the soluble hIAPP species. Deamidation was observed in the day-7, day-14, day-21, and day-28 samples (Fig. 2B). On day-7, ~7.5% of the y_5 fragment ion was deamidated while no deamidation was observed for the b_{21} and b_{22} fragment ions in the pellet. On day-14, the extent of deamidation for the y_5 fragment ion increased sharply to 16% and the b21 and b22 showed ~7.5% deamidation. After 28 days incubation, the extent of deamidation of the y_5, b_{21}, and b_{22} fragment ions were at 39%, 30%, and 29% respectively, distinctly larger than for the soluble hIAPP species above, suggesting the fibrils of hIAPP contains a higher extent of deamidation at Asn-35 compared to Asn-21 and Asn-22 residues. The residue Asn-35 was the earliest deamidation site observed in the incubated solutions and contained the highest extent of deamidation in the fibril pellets, which agrees with the findings in previous deamidation studies,[3, 31] suggesting that the primary sequence of Ser-[35]Asn-Thr in hIAPP had the shortest deamidation time among all the other segments studied. The higher extent of deamidation observed in the fibrils of hIAPP compared to the incubated solutions also indicates that deamidated hIAPP tends to aggregate and form insoluble fibrils more rapidly than the wild-type hIAPP.
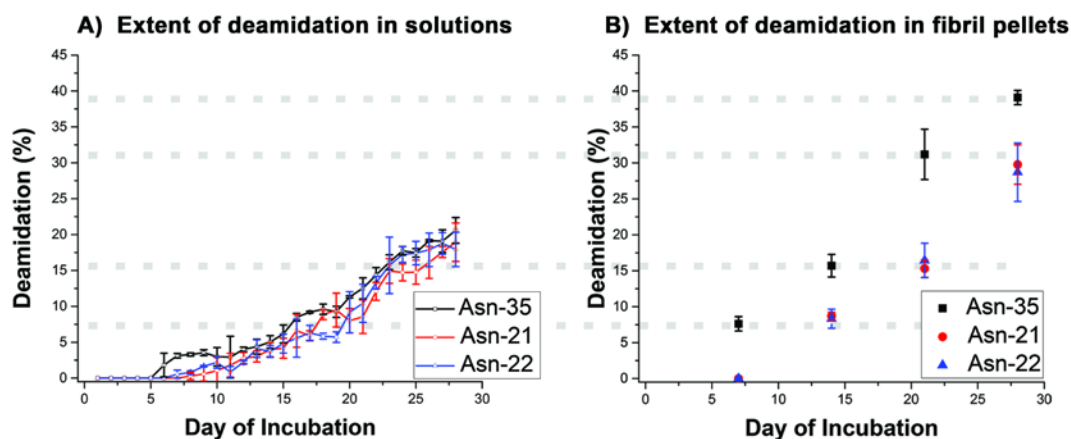
Figure 2. The extent of deamidation observed in CAD MS/MS fragments; the y_5 (black), b_{21} (red), and

b_{22} (blue) for 10 μM aqueous hIAPP (A) solutions and (B) dissolved fibril solutions.

In order to ascertain the effects of deamidated isomeric products on the aggregation process, pure mutant hIAPP peptides were synthesised with aspartic acid ((D)₃hIAPP) or iso-aspartic acid ((isoD)₃hIAPP) replacement at the detected deamidation site from above, i.e. residues 21, 22, and 35 (Fig. S1, ESI†). The 7+ charge state dimers of ((D)₃hIAPP) and ((isoD)₃hIAPP) were fragmented by ECD MS/MS in order to determine the non-covalent interaction region between the mutant hIAPP units (Fig. S2 – S3, ESI†). The aggregation regions of ((D)₃hIAPP) and ((isoD)₃hIAPP) were found between Asn-31 and Thr-36 residues, which is similar to the proposed aggregation region of 7+ charge state dimer of wild-type hIAPP in the previous studies, suggesting there is no difference between the wild-type and the two mutant hIAPPs regarding the aggregation sites for the formation of early oligomers.[32]

MS can quantify soluble amyloid proteins in solution.[32] The ionisation of aqueous protein solutions to gas phase ions, however, is limited to soluble components only, so that the insoluble fibrils are difficult to quantify using MS. Thus, the relative concentration of amyloid fibrils formed in the incubated solutions were determined by using Thioflavin T (ThT) fluorescence emission analysis at the wavelength of 490 nm and the overall structures of fibrils were observed using transmission electron microscopy (TEM). The relative fluorescence emission of the 10 μM solutions of wild-type hIAPP, ((D)₃hIAPP), and ((isoD)₃hIAPP) were measured and the lag phases of the formation of mature fibrils in wild-type hIAPP solution was 42 hours while in ((D)₃hIAPP) and ((isoD)₃hIAPP) solutions were ~ 30 hours (Fig. 3A – 3C), indicating mutant hIAPPs with deamidated residues replacement at Asn-21, Asn-22, and Asn-35 accelerate the rate of mature fibrils formation which supports the hypothesis that deamidated hIAPPs accelerate the aggregation rate of non-deamidated hIAPP.[18, 19] TEM images of the wild-type hIAPP, ((D)₃hIAPP), and ((isoD)₃hIAPP) solutions incubated at 37°C for one week were also obtained (Fig. 3E – 3G). Branched and elongated fibrils were observed in the wild-type hIAPP as well as ((D)₃hIAPP) incubated solutions; while densely packed fibrils were found in ((isoD)₃hIAPP) solution. The fibril structures observed in ((isoD)₃hIAPP) solution were distinctly different from the fibrils found in wild-type hIAPP and ((D)₃hIAPP), suggesting the morphology of fibrils formed in ((isoD)₃hIAPP) is different from wild-type hIAPP as well as ((D)₃hIAPP).
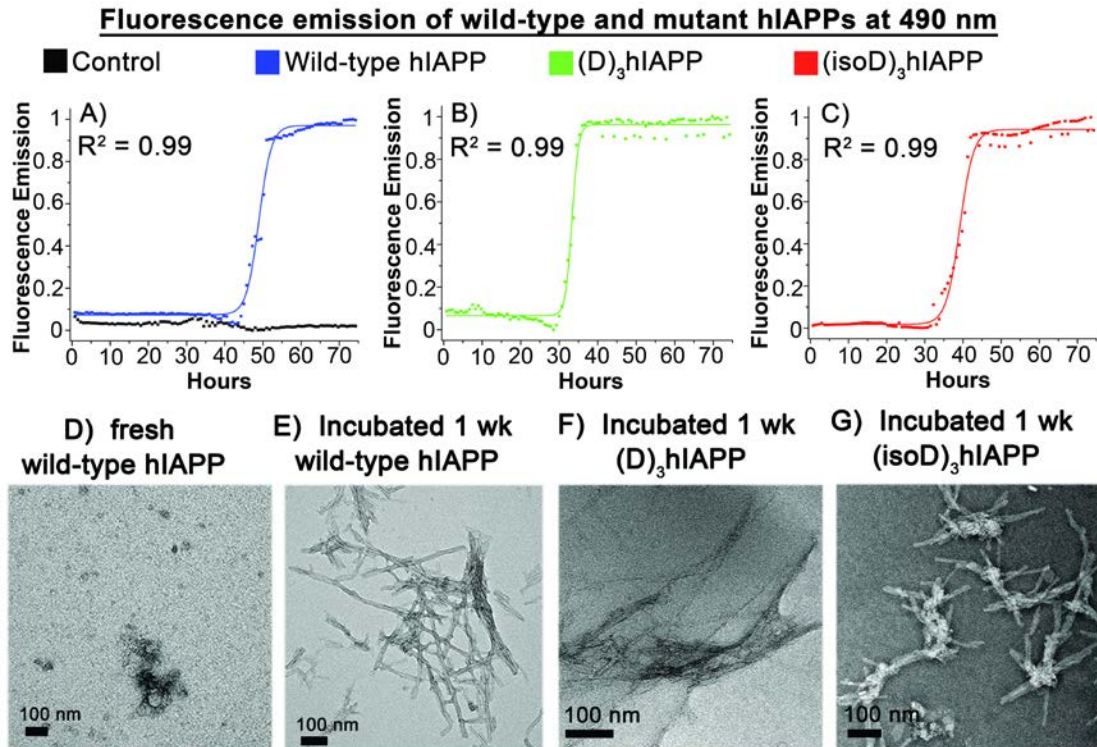
Figure 3. The relative fluorescence activity of the incubated 10 μM (A) ThT solution (control; black), 10 μM wild-type hIAPP (blue), (B) 10 μM mutant ((D)$_3$hIAPP) (green), and (C) 10 μM mutant ((isoD)$_3$hIAPP) (red) solutions measured at emission 490 nm. The TEM images of the (D) fresh and (E) 1-week incubated 10 μM wild-type hIAPP solutions. The TEM images of 10 μM (F) ((D)$_3$hIAPP) and (G) ((isoD)$_3$hIAPP) solutions after 1 week incubation at 37$^{\text{o}}$C. The scale bars for each TEM image are inset.

In order to study the effects of the isomeric deamidation products on the wild-type hIAPP aggregation, ((D)$_3$hIAPP) and ((isoD)$_3$hIAPP) solutions were individually spiked into wild-type hIAPP solution at 5%, 10%, 25%, and 50% amounts. After one week incubation, the percentage of remaining soluble monomeric hIAPP in the seeded solutions was consistently less in the spiked solutions than the control hIAPP incubated solution, and less soluble hIAPP was found in the mutant ((isoD)$_3$hIAPP) spiked solutions compared to the ((D)$_3$hIAPP) spiked solutions (Fig. 4A). The p-values of seeding 5% and 10% mutant ((D)$_3$hIAPP) into the solution were higher than 0.05, which indicated the differences between the seeded solutions and the control sample were not significant. The p-values of the remaining seeded solutions were less than 0.05, which showed significant differences between the control and the seeded solutions. The normalised percentage of soluble hIAPP with 5% spiking of ((D)$_3$hIAPP) or ((isoD)$_3$hIAPP) was 4% and 9% less than the soluble hIAPP found in the control incubated solutions respectively. The normalised percentage of soluble hIAPP consistently decreased with increased

amounts of ((D)₃hIAPP) or ((isoD)₃hIAPP) in the incubated solutions. For the solutions with 50% spiking of ((D)₃hIAPP) or ((isoD)₃hIAPP), the normalised percentage of soluble hIAPP was 28% and 46% less than the soluble hIAPP found in the control solutions respectively. These results indicate the effects of mutant hIAPPs in accelerating wild-type hIAPP are concentration-dependent.
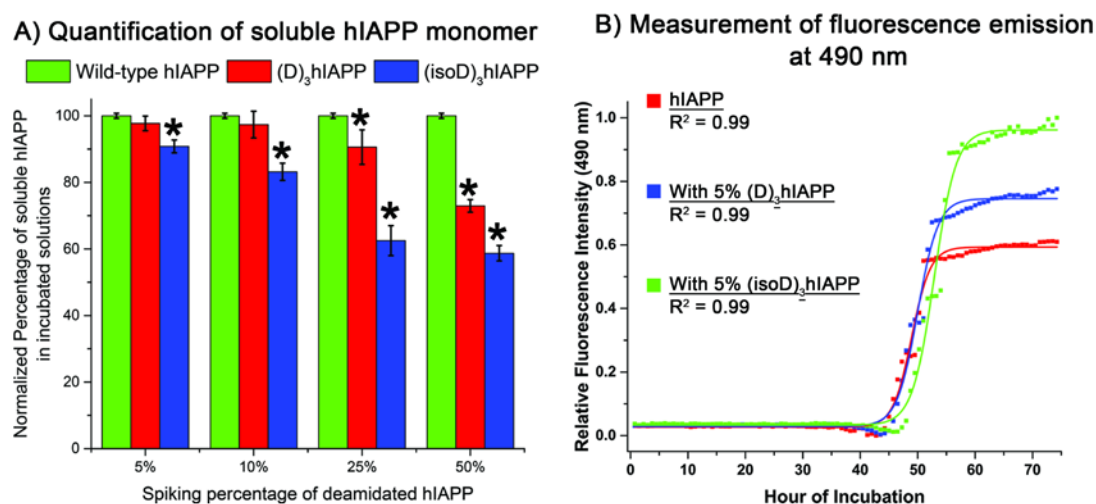
Figure 4. (A) A plot showing the normalised percentage of soluble hIAPP in the 10 μM solutions with spiking different percentage of mutant ((D)₃hIAPP) or ((isoD)₃hIAPP) to wild-type hIAPP (control) measured using MS after 1 week incubation. * indicates the p-value of the sample percentages are less than 0.05 compared to the control percentage in a paired t-test. (D) The relative fluorescence activity of 10 μM hIAPP, 9.5 μM hIAPP plus 0.5 μM (5%) ((D)₃hIAPP), and 9.5 μM hIAPP plus 0.5 μM (5%) ((isoD)₃hIAPP) measured at emission 490 nm.

The fibrils formed during the incubation experiments were measured using ThT fluorescence spectroscopy. The measured percentage change of fluorescence emission in 5% mutant hIAPP seeded solutions further indicated that the amount of amyloid fibrils formed in the seeded solutions were consistently higher than the wild-type hIAPP incubated solution and the overall percentage of amyloid fibrils formed in ((D)₃hIAPP) and ((isoD)₃hIAPP) seeded solutions was 27% and 48% higher than the wild-type hIAPP incubated solution respectively (Fig. 4B). The fluorescence emission measurement and MS quantification showed the effect of seeding ((isoD)₃hIAPP) is twice that of seeding the same amount of ((D)₃hIAPP) into non-deamidated hIAPP solutions. The difference between the TEM images of incubated ((D)₃hIAPP) and ((isoD)₃hIAPP) solutions also agrees the greater effect of ((isoD)₃hIAPP) compared to ((D)₃hIAPP) (Fig. 3E – 3G). The observed morphology of fibrils was different in ((isoD)₃hIAPP) compared to ((D)₃hIAPP), indicating differences in the aggregation behaviour and rate of non-deamidated hIAPP, as observed in the MS and fluorescence.

7

In order to examine the effects of mutant ((D)$_3$hIAPP) and ((isoD)$_3$hIAPP) in incubated solutions and fibrillary pellets, MS spectra of mixed wild-type hIAPP with various spiking percentage of mutant ((D)$_3$hIAPP) and ((isoD)$_3$hIAPP) were acquired (Fig. S4, ESI†).   The peak intensity of mutant ((D)$_3$hIAPP) and ((isoD)$_3$hIAPP) were consistently higher in the fibrillary pellets compared to the incubated and the fresh solutions, suggesting the important role of ((D)$_3$hIAPP) or ((isoD)$_3$hIAPP) in enhancing fibril formation.

The experimental results herein demonstrate the importance as well as the effects of hIAPP deamidation on hIAPP aggregation rate.   Deamidation of hIAPP is shown to occur at Asn-21, Asn-22, as well as Asn-35 residues of the incubation and a higher percentage of deamidated hIAPP was observed in fibrillary pellet, suggesting that deamidated hIAPP can accelerate the rate of hIAPP fibril formation.   The experimental results of the mutant hIAPP, ((D)$_3$hIAPP) and ((isoD)$_3$hIAPP), not only agree with the hypothesis of deamidated hIAPP can increase fibril formation, but also suggest the effect of seeding ((isoD)$_3$hIAPP) is twice than that of ((D)$_3$hIAPP) seeding into non-deamidated hIAPP solutions as the morphology of ((isoD)$_3$hIAPP) fibrils are distinctly different from the fibrils formed in ((D)$_3$hIAPP) solutions.   These results provide qualitative and quantitative evaluation of deamidated hIAPP on the rate of aggregation which could help inform further studies of the effects of deamidation on accelerating amyloid fibril formation.

Conflicts of interest

There are no conflicts to declare.

Acknowledgements

References

1.   E. R. Stadtman, *J. Gerontol.*, 1988, **43**, B112-B120.
2.   J. J. Cournoyer, J. L. Pittman, V. B. Ivleva, E. Fallows, L. Waskell, C. E. Costello and P. B. O'Connor, *Protein Sci.*, 2005, **14**, 452-463.
3.   N. E. Robinson and A. B. Robinson, *Proc. Natl. Acad. Sci. USA*, 2001, **98**, 944-949.
4.   A. B. Robinson and C. J. Rudd, *Curr. Top. Cell. Regul.*, 1974, **8**, 247-295.
5.   H. T. Wright, *Crit. Rev. Biochem. Mol. Biol.*, 1990, **26**, 1-52.

6. H. A. Doyle and M. J. Mamula, *Trends Immunol.*, 2001, **22**, 443-449.

7. N. E. Robinson and A. Robinson, *Molecular clocks: deamidation of asparaginyl and glutaminyl residues in peptides and proteins*, Althouse press, Oregon, 2004.

8. N. P. Sargaeva, C. Lin and P. B. O'Connor, *Anal. Chem.*, 2011, **83**, 6675-6682.

9. T. Shimizu, H. Fukuda, S. Murayama, N. Izumiyama and T. Shirasawa, *J. Neurosci. Res.*, 2002, **70**, 451-461.

10. N. M. Kad, N. H. Thomson, D. P. Smith, D. A. Smith and S. E. Radford, *J. Mol. Biol.*, 2001, **313**, 559-571.

11. A. J. Soulby, J. W. Heal, M. P. Barrow, R. A. Roemer and P. B. O'Connor, *Protein Sci.*, 2015, **24**, 850-860.

12. R. Gupta and O. P. Srivastava, *Invest. Ophthalmol. Vis. Sci.*, 2004, **45**, 206-214.

13. T. Takata, J. T. Oxford, B. Demeler and K. J. Lampi, *Protein Sci.*, 2008, **17**, 1565-1575.

14. G. J. S. Cooper, A. J. Day, A. C. Willis, A. N. Roberts, K. B. M. Reid and B. Leighton, *Biochim. Biophys. Acta*, 1989, **1014**, 247-258.

15. E. Jaikaran, M. R. Nilsson and A. Clark, *Biochem. J*, 2004, **377**, 709-716.

16. S. Luca, W. M. Yau, R. Leapman and R. Tycko, *J. Biochem.*, 2007, **46**, 13505-13522.

17. G. T. Westermark, P. Westermark, C. Berne, O. Korsgren and T. Nordic Network Clin Islet, *New Engl. J. Med.*, 2008, **359**, 977-979.

18. M. R. Nilsson, M. Driscoll and D. P. Raleigh, *Protein Sci.*, 2002, **11**, 342-349.

19. E. B. Dunkelberger, L. E. Buchanan, P. Marek, P. Cao, D. P. Raleigh and M. T. Zanni, *J. Am. Chem. Soc.*, 2012, **134**, 12658-12667.

20. L. Haataja, T. Gurlo, C. J. Huang and P. C. Butler, *Endocr. Rev.*, 2008, **29**, 303-316.

21. A. Clark, C. Wells, I. Buley, J. Cruickshank, R. Vanhegan, D. Matthews, G. Cooper, R. Holman and R. Turner, *Diabetes research (Edinburgh, Scotland)*, 1988, **9**, 151-159.

22. A. Lorenzo, B. Razzaboni, G. C. Weir and B. A. Yankner, *Nature*, 1994, **368**, 756-760.

23. K. Potter, A. Abedini, P. Marek, A. Klimek, S. Butterworth, M. Driscoll, R. Baker, M. Nilsson, G. Warnock and J. Oberholzer, *Proc. Natl. Acad. Sci. USA*, 2010, **107**, 4305-4310.

24. P. T. Nguyen, X. Zottig, M. Sebastiao and S. Bourgault, *J. Biochem.*, 2017, **56**, 3808-3817.

25. R. Akter, P. Cao, H. Noor, Z. Ridgway, L. H. Tu, H. Wang, A. G. Wong, X. X.

Zhang, A. Abedini, A. M. Schmidt and D. P. Raleigh, *J. Diabetes Res.*, 2016, DOI: 10.1155/2016/2798269, 18.

26.   W. Y. K. Chan, T. D. Chan and P. B. O'Connor, *J. Am. Soc. Mass. Spectrom.*, 2010, **21**, 1012-1015.

27.   P. P. Hurtado and P. B. O'Connor, *Anal. Chem.*, 2012, **84**, 3017-3025.

28.   X. Li, X. Yu, C. E. Costello, C. Lin and P. B. O'Connor, *Anal. Chem.*, 2012, **84**, 6150-6157.

29.   J. J. Cournoyer, C. Lin, M. J. Bowman and P. B. O'Connor, *J. Am. Soc. Mass. Spectrom.*, 2007, **18**, 48-56.

30.   H. Yang and R. A. Zubarev, *Electrophoresis*, 2010, **31**, 1764-1772.

31.   N. E. Robinson and A. B. Robinson, *Proc. Natl. Acad. Sci. U. S. A.*, 2001, **98**, 4367-4372.

32.   Y. P. Y. Lam, C. A. Wootton, I. Hands-Portman, J. Wei, C. K. C. Chiu, I. Romero-Canelon, F. Lermyte, M. P. Barrow and P. B. O'Connor, *Anal. Chem.*, 2018, **Submitted**.

33.   P. Caravatti and M. Allemann, *Org. Mass Spectrom.*, 1991, **26**, 514-518.

34.   F. T. S. Chan, G. S. K. Schierle, J. R. Kumita, C. W. Bertoncini, C. M. Dobson and C. F. Kaminski, *Analyst*, 2013, **138**, 2156-2162.

35.   T. Yang, X. H. Wang, C. L. Zhang, X. Ma, K. Wang, Y. Q. Wang, J. Luo, L. Yang, C. Yao and X. Y. Wang, *Chem. Commun.*, 2016, **52**, 2245-2248.
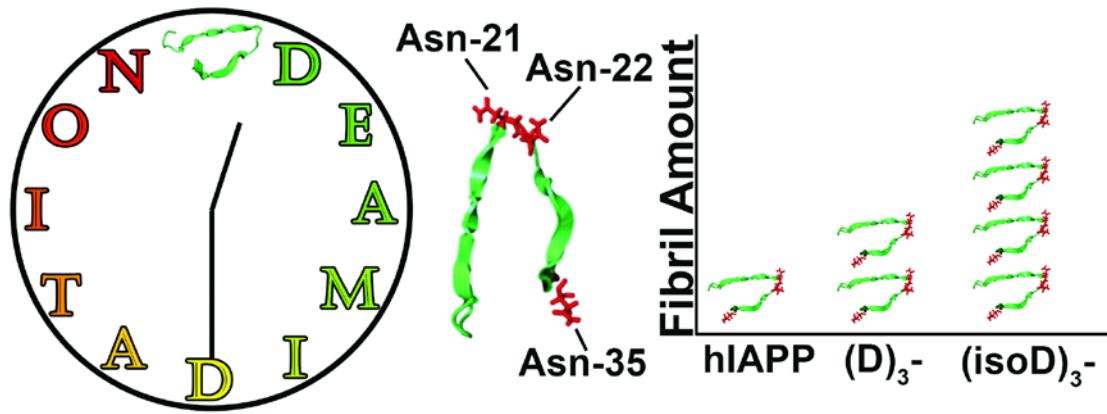
Graphic Abstracts:

Deamidation sites of hIAPP were determined and the amount of fibril formed in mutant hIAPPs were higher than wild-type hIAPP.

Electronic Supplementary Information

Experimental Procedure

Sample preparation for deamidated hIAPP and fibrils. Wild-type hIAPP lyophilized powder (Sigma Aldrich Company Ltd, Dorset, England) was dissolved in Milli-Q (Direct-Q® 3 UV System, Millipore Corporation, US) H_2O (~pH 7.5) at a concentration of 500 µM and further diluted into 10 uM solution. The 10 µM hIAPP aqueous solution was incubated for 28 days (4 weeks). The incubated solution was then centrifuged at 14,000 rpm for one hour to separate the soluble hIAPP (supernatant) from the insoluble hIAPP fibril (fibrillary pellet). The supernatant solution containing soluble hIAPP was then diluted 20-fold with 49.5:49.5:1 water/acetonitrile/formic acid prior to MS analysis. hIAPP fibrillary pellets from 7-, 14-, 21-, and 28-day solutions were rinsed with 100 µL Milli-Q H_2O three times and then re-dissolved with 20 µL of 47.5:47.5:5 water/acetonitrile/formic acid, and sonicated in water bath at 37 °C for one hour. Re-dissolved samples were further diluted with 80 µL of 50:50 water/acetonitrile. The final concentration of formic acid in solutions was 1% (mol/mol).

Sample preparation for seeding mutant peptides. Wild-type hIAPP lyophilized powder and synthetic mutant hIAPPs (Pepscan Company Ltd, The Netherlands) were dissolved in Milli-Q H_2O to a concentration of 500 µM. The seeding experiments were performed by mixing wild-type hIAPP stock solution with 5%, 10%, 25%, or 50% mutant ((D)$_3$hIAPP) or ((isoD)$_3$hIAPP) solutions. Samples were then diluted to a final concentration of 10 µM wild-type hIAPP plus mutant ((D)$_3$hIAPP) or ((isoD)$_3$hIAPP), which were incubated for 1 week at 37°C. The supernatants and fibrillary pellets were separated and prepared as mentioned above.

FTICR MS analysis. Mass spectra were acquired on a 12 tesla solariX FTICR MS (Bruker Daltonik GmbH, Bremen, Germany). All samples were analyzed in positive ionization mode. For the detection of deamidated hIAPP and dissociated fibrils, an Apollo II electrospray ionization (ESI) source (Bruker Daltonik GmbH, Bremen, Germany) was used with a capillary voltage of 4-4.5 kV. The ESI flow rate was optimized to 100-150 µL/h and the source temperature was set to 200°C. Ions were externally accumulated in a hexapole collision cell before transferred to an infinity cell (ICR cell) for excitation and detection.[33] Data obtained from FTICR-MS were analyzed using Bruker DataAnalysis 4.2 software (Bruker Daltonics, Bremen, Germany). For the CAD experiments, precursor ions were first isolated using the quadrupole mass filter, then collided with argon gas and accumulated in the collision cell. The collision energy was optimized to 2-18 V and the ion accumulation time to

1-3 seconds.   Fragments were then transferred to the infinity cell for detection.   The most intense isotopic peak from each fragment with signal-to-noise ratio (S/N) over 5 was manually matched with the theoretical *m/z*.   All of the fragments were internally calibrated and then assigned with an uncertainty less than 1 part-per-million (ppm).

Quantification of deamidated/ mutant hIAPP in solutions and fibrillary pellets. The monoisotopic peak area of non-deamidated and deamidated/mutant hIAPP peaks were measured using Bruker DataAnalysis 4.2 software.   The percentage of deamidated hIAPP (%) was calculated as follows:

$$\text{Deamidated (\%)} = \frac{Peak\ area\ of\ deamidated\ hIAPP}{Sum\ of\ Peak\ area\ of\ deamidated\ hIAPP\ and\ nondeamidated\ hIAPP}\ x\ 100\%$$

The same calculation method was applied to obtain the percentage of mutant hIAPP against wild-type hIAPP.

Transmission electron microscopy (TEM).   The TEM images of the incubated solutions, including 10 µM wild-type hIAPP, 10 µM mutant ((D)$_3$hIAPP), and 10 µM mutant ((isoD)$_3$hIAPP) solution were acquired on a Jeol 2010F TEM operated at 200 kV.   10 µL of incubated solution was transferred onto a carbon-coated grid and settled for one minute, followed by removing the excess solution using filter paper. A 2% (w/v) uranyl acetate solution was used for the negative stain. Multiple images with magnification from x10,000 to x40,000 were acquired.

Thioflavin T (ThT) fluorescence reactivity.   The fluorescence reactivity of the 10 µM hIAPP, mutant ((D)$_3$hIAPP), mutant ((isoD)$_3$hIAPP), and hIAPP seeding solutions were measured using a GloMax®-Multi Detection System (Promega; Wisconsin, USA).   All samples were placed in a black 96 well-plate and mixed with 10 µM ThT aqueous solution.   Fluorescence spectra of the samples were acquired every 45 minutes with excitation at 405 nm and emission measurement at 490 nm, in a similar fashion to Chan *et al.*[34, 35]   The intensities obtained from the fluorescence spectrometer were normalized to the signal intensity of the most mature fibril.

Deamidated (D)₃hIAPP: KCNTATCATQ RLANFLVHSS DDFGAILSST NVGSDTY-NH$_2$

Deamidated (isoD)₃hIAPP: KCNTATCATQ RLANFLVHSS (isoD)(isoD)FGAILSST NVGS(isoD)TY-NH$_2$

Figure S1. Sequences of synthetic mutant hIAPPs. Asn residues at position 21, 22, and 35 are replaced with aspartic acid – deamidated ((D)₃hIAPP) or iso-aspartic acid – deamidated ((isoD)₃hIAPP) in order to act as deamidation mimics.
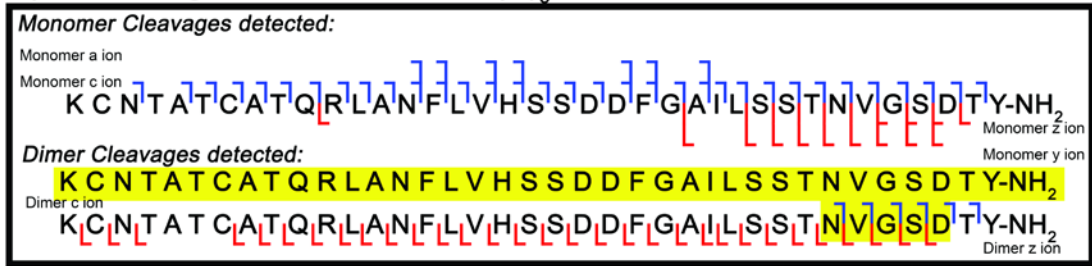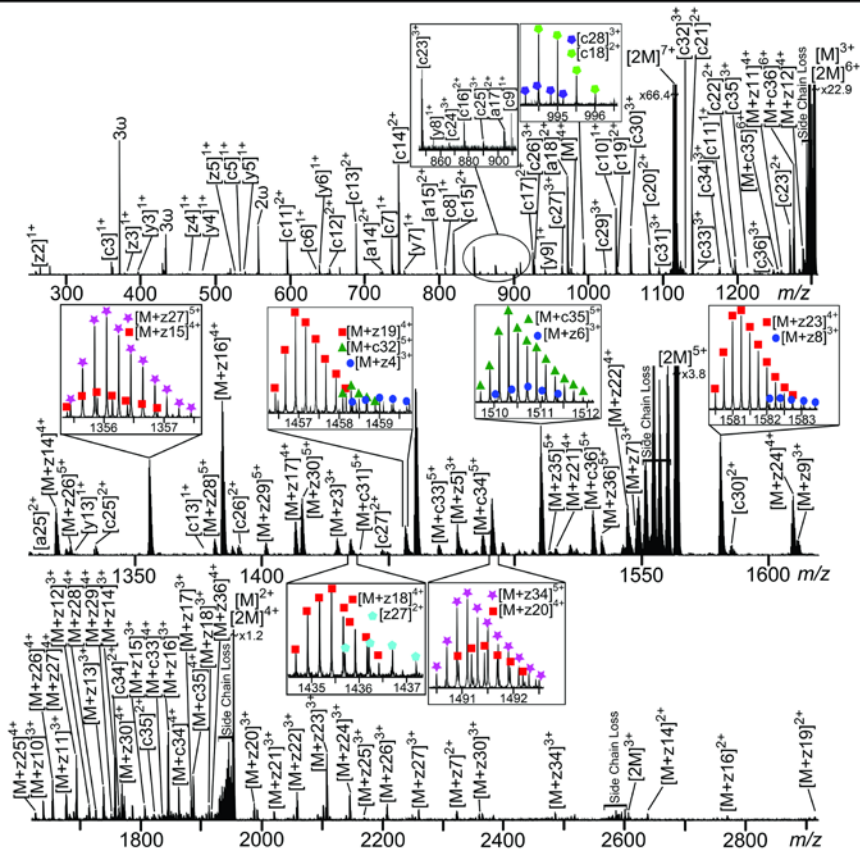
Figure S2. (A) Summary of a-, c-, y-, and z-ion fragments observed in the (B) ECD MS/MS spectrum of the 7+ charge state ((D)$_3$hIAPP) dimer. Highlighted sequence represents the proposed non-covalent interaction region. The side chain losses were not labeled for clarity. The assigned fragments are listed in the ESI Table S1.

Assignment Table of the ECD MS/MS of
7+ charge state ((D)₃hIAPP) dimer

Ion	charge	Theoretical m/z	Experimental m/z	Error (ppm)
MH	4+	977.462474	977.461786	-0.704
MH	3+	1302.279143	1302.279165	0.017
MH	2+	1952.915077	1952.915991	0.468
2[MH]	7+	1116.383162	1116.383047	-0.103
2[MH]	6+	1303.115465	1303.115560	0.073
2[MH]	5+	1563.738667	1563.738999	0.212
2[MH]	4+	1954.673471	1954.674185	0.365
2[MH]	3+	2605.897413	2605.897274	-0.053
a14	2+	724.354565	724.354485	-0.110
a15	2+	797.888772	797.888565	-0.259
a17	2+	903.965011	903.965096	0.094
a18	2+	972.494467	972.494518	0.052
a22	2+	1174.553438	1174.553758	0.272
a23	2+	1248.087645	1248.088012	0.294
a25	2+	1312.116934	1312.116940	0.005
c3	1+	362.173076	362.173008	-0.188
c5	1+	534.257869	534.257735	-0.251
c6	1+	636.313372	636.313252	-0.189
c7	1+	737.306908	737.306867	-0.056
c8	1+	808.344022	808.344002	-0.025
c9	1+	909.391701	909.391767	0.073
c10	1+	1037.450279	1037.450336	0.055
c11	2+	597.279333	597.279236	-0.162
c11	1+	1193.551390	1193.551711	0.269
c12	2+	653.821365	653.821279	-0.132
c13	2+	689.339922	689.339851	-0.103
c13	1+	1377.672568	1377.673273	0.512
c14	2+	746.361386	746.361348	-0.051
c15	2+	819.895593	819.895538	-0.067
c16	2+	876.437625	876.437608	-0.019
c17	2+	925.971832	925.971879	0.051
c18	2+	994.501288	994.501285	-0.003
c19	2+	1038.017303	1038.017350	0.045
c20	2+	1081.533317	1081.533397	0.074
c21	2+	1139.046789	1139.046866	0.068
c22	2+	1196.560261	1196.560497	0.197
c23	3+	847.065404	847.065401	-0.004
c23	2+	1270.094468	1270.094648	0.142
c24	3+	866.072559	866.072757	0.229
c25	3+	889.751597	889.751369	-0.256
c25	2+	1334.123849	1334.123808	-0.031
c26	3+	927.446285	927.446297	0.013
c26	2+	1390.665789	1390.665948	0.114
c27	3+	965.140973	965.141253	0.290
c27	2+	1447.709221	1447.709709	0.337
c28	3+	994.151649	994.151665	0.016
c29	3+	1023.162325	1023.162402	0.075
c29	2+	1535.242655	1535.243476	0.535
c30	3+	1056.844885	1056.844929	0.042
c30	2+	1584.763690	1584.764560	0.549
c31	3+	1094.859194	1094.859257	0.058
c31	2+	1642.286550	1642.287622	0.653
c32	3+	1127.881999	1127.882005	0.005
c32	2+	1692.823617	1692.824904	0.760
c33	3+	1146.889154	1146.889155	0.001
c34	3+	1175.899830	1175.899842	0.010
c34	2+	1763.347107	1763.347520	0.801
c35	3+	1214.576411	1214.576892	0.396
c35	2+	1820.859579	1820.859860	0.154
c36	3+	1247.924704	1247.924446	-0.207
y3	1+	397.171777	397.171687	-0.227
y4	1+	484.203806	484.203654	-0.314
y5	1+	541.225270	541.225155	-0.212
y6	1+	640.293684	640.293629	-0.086
y7	1+	754.336612	754.336600	-0.016
y8	1+	855.384291	855.384408	0.137
y9	1+	942.416320	942.416439	0.126
y10	1+	1029.448349	1029.448387	0.037
y13	1+	1326.653591	1326.653604	0.010
z2	1+	266.126109	266.126109	0.000
z3	1+	382.160877	382.160842	-0.092
z4	1+	467.177255	467.177105	-0.321
z5	1+	526.214369	526.214234	-0.257
z27	2+	1435.701402	1435.700996	-0.283
M+c31	5+	1438.883524	1438.884166	0.446
M+c32	5+	1458.496774	1458.496281	-0.338
M+c32	4+	1822.618557	1822.618598	0.022
M+c33	5+	1469.700594	1469.701214	0.422
M+c33	4+	1837.376472	1837.376990	0.282
M+c34	5+	1487.107000	1487.107008	0.005
M+c34	4+	1858.883887	1858.885137	0.672
M+c35	6+	1258.761936	1258.761197	-0.587
M+c35	5+	1510.312868	1510.313214	0.229
M+c35	4+	1887.891222	1887.892061	0.444
M+c36	6+	1275.603219	1275.603240	0.016
M+c36	5+	1530.924420	1530.924741	0.210
M+z3	3+	1429.328685	1429.329245	0.392
M+z4	3+	1458.339361	1458.339574	0.079
M+z5	3+	1477.346514	1477.347034	0.352
M+z6	3+	1510.369320	1510.368816	-0.334
M+z7	3+	1548.049351	1548.049768	0.269
M+z7	2+	2323.077144	2323.078314	0.504
M+z8	3+	1582.400354	1582.401276	0.583
M+z9	3+	1611.746974	1611.746129	-0.524
M+z10	3+	1639.753258	1639.752527	-0.446
M+z11	4+	1258.839125	1258.839009	-0.092
M+z11	3+	1677.447952	1677.448418	0.278
M+z12	4+	1287.110147	1287.110616	0.364
M+z12	3+	1715.811104	1715.812415	0.764
M+z13	4+	1304.869427	1304.869520	0.071
M+z13	3+	1738.821678	1738.820724	-0.549
M+z14	4+	1318.623443	1318.623618	0.133
M+z14	3+	1757.828832	1757.829443	0.348
M+z14	2+	2637.748852	2637.749391	0.204
M+z15	4+	1355.390547	1355.390850	0.224
M+z15	3+	1807.856058	1807.856916	0.475
M+z16	4+	1384.147283	1384.147298	0.011
M+z16	3+	1846.532522	1846.533255	0.397
M+z16	2+	2769.799453	2769.799567	0.041
M+z17	4+	1412.904019	1412.904502	0.342
M+z17	3+	1884.874843	1884.874962	0.063
M+z18	4+	1434.912737	1434.913034	0.207
M+z18	3+	1913.885523	1913.885817	0.154
M+z19	4+	1456.420033	1456.420138	0.072
M+z19	3+	1942.896202	1942.895513	-0.355
M+z19	2+	2914.846456	2914.846774	0.109
M+z20	4+	1491.186124	1491.186700	0.386
M+z20	3+	1988.582507	1988.583390	0.444
M+z21	4+	1515.953231	1515.953433	0.133
M+z21	3+	2021.605320	2021.606146	0.409
M+z22	4+	1544.224252	1544.224820	0.368
M+z22	3+	2059.300020	2059.301231	0.588
M+z23	4+	1580.489984	1580.490360	0.238
M+z23	3+	2108.322843	2108.323867	0.486
M+z24	4+	1609.000716	1609.001073	0.222
M+z24	3+	2146.337153	2146.338370	0.567
M+z25	4+	1627.512008	1627.512728	0.442
M+z25	3+	2170.350335	2170.351553	0.561
M+z26	5+	1324.827880	1324.828098	0.165
M+z26	4+	1655.783031	1655.783641	0.368
M+z26	3+	2208.046833	2208.046628	-0.093
M+z27	5+	1356.048099	1356.048275	0.130
M+z27	4+	1695.060261	1695.060689	0.252
M+z27	3+	2260.080530	2260.081089	0.247
M+z28	5+	1381.659815	1381.660080	0.192
M+z28	4+	1726.824267	1726.824613	0.200
M+z29	5+	1402.069844	1402.070205	0.257
M+z29	4+	1752.086188	1752.086770	0.332
M+z30	5+	1416.076777	1416.077014	0.167
M+z30	4+	1770.096109	1770.096483	0.211
M+z30	3+	2359.792401	2359.792212	-0.080
M+z34	5+	1491.103517	1491.103695	0.119
M+z34	4+	1864.130123	1864.130663	0.290
M+z34	3+	2485.507093	2485.507949	0.344
M+z35	5+	1513.912103	1513.912030	-0.048
M+z36	5+	1534.713228	1534.713352	0.081
M+z36	4+	1918.141132	1918.141936	0.419

Average Error:	0.124	
Absolute Average Error:	0.236	
Standard Deviation:	0.278	

Table S1. List of the assigned fragments from the ECD MS/MS spectrum of the 7+ charge state ((D)₃hIAPP) dimer ion. M represents one ((D)₃hIAPP) unit.
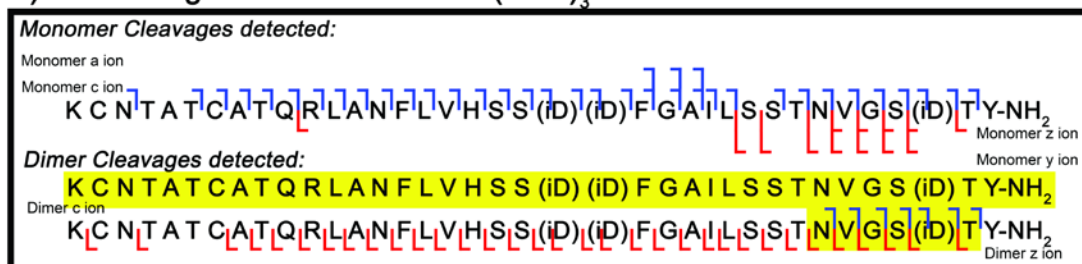
Figure S3. (A) Summary of a-, c-, y-, and z-ion fragments observed in the (B) ECD MS/MS spectrum of the 7+ charge state ((isoD)$_3$hIAPP) dimer. Highlighted sequence represents the proposed non-covalent interaction region. The side chain losses were not labeled for clarity. The assigned fragments are listed in the ESI Table S2.
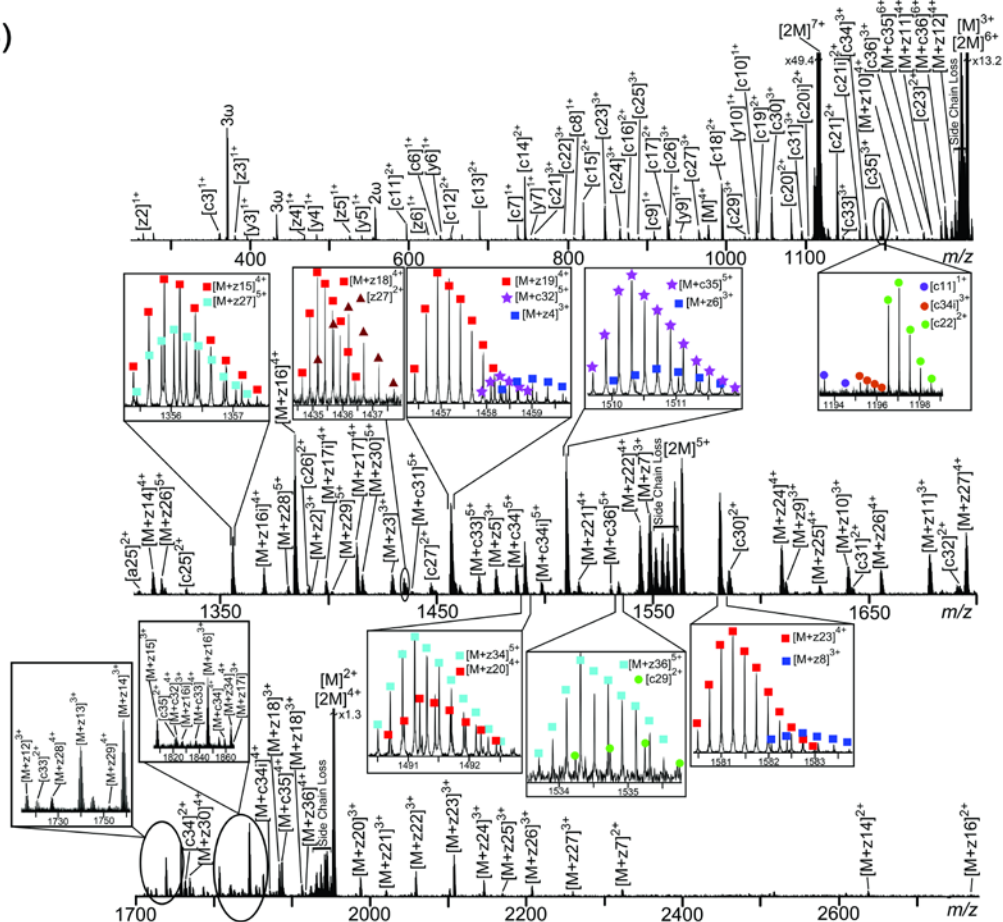
Assignment Table of the ECD MS/MS of 7+ charge state ((isoD)$_3$hIAPP) dimer

Type	Ion	charge	Theoretical m/z	Experimental m/z	Error (ppm)
MH	MH	4+	977.211884	977.211677	-0.212
MH	MH	3+	1302.279143	1302.279080	-0.048
MH	MH	2+	1952.915077	1952.915655	0.296
2[MH]	2[MH]	7+	1116.383162	1116.383218	0.050
2[MH]	2[MH]	6+	1303.115465	1303.115597	0.101
2[MH]	2[MH]	5+	1563.738667	1563.738713	0.029
2[MH]	2[MH]	4+	1954.673471	1954.672757	-0.365
a	23	2+	1248.087645	1248.087793	0.119
a	24	2+	1277.099772	1277.099889	0.092
a	25	2+	1312.116934	1312.117109	0.133
c	3	1+	362.173076	362.173033	-0.119
c	6	1+	636.313372	636.313275	-0.152
c	7	1+	737.306908	737.306876	-0.043
c	8	1+	808.344022	808.343966	-0.069
c	9	1+	909.391701	909.391605	-0.106
c	10	1+	1037.450279	1037.450277	-0.002
c	11	2+	597.279333	597.279315	-0.030
c	11	1+	1193.551390	1193.551247	-0.120
c	12	2+	653.821365	653.821303	-0.095
c	13	2+	689.339922	689.339931	0.013
c	14	2+	746.361386	746.361372	-0.019
c	15	2+	819.895593	819.895597	0.005
c	16	2+	876.437625	876.437697	0.082
c	17	2+	925.971832	925.971846	0.015
c	18	2+	994.501288	994.501292	0.004
c	19	2+	1038.017303	1038.017376	0.070
c	20	2+	1081.533317	1081.533351	0.031
c	21	3+	759.700285	759.700251	-0.045
c	21	2+	1139.046789	1139.046820	0.027
c	22	3+	798.042599	798.042537	-0.078
c	22	2+	1196.560261	1196.560293	0.027
c	23	3+	847.065404	847.065386	-0.021
c	23	2+	1270.094468	1270.094418	-0.039
c	24	3+	866.072559	866.072652	0.107
c	25	3+	889.751597	889.751696	0.111
c	25	2+	1334.123849	1334.123757	-0.069
c	26	3+	927.446285	927.446286	0.001
c	26	2+	1390.665789	1390.666501	0.512
c	27	3+	965.140973	965.140963	-0.010
c	27	2+	1447.709221	1447.709778	0.385
c	29	3+	1023.162325	1023.162215	-0.108
c	29	2+	1534.239850	1534.239965	0.075
c	30	3+	1056.844885	1056.844848	-0.035
c	30	2+	1584.763690	1584.763724	0.021
c	31	3+	1094.859194	1094.859270	0.069
c	31	2+	1642.787956	1642.788594	0.388
c	32	3+	1127.881999	1127.881584	-0.368
c	32	2+	1691.319356	1691.320699	0.794
c	33	3+	1146.889154	1146.888901	-0.221
c	33	2+	1720.331490	1720.332143	0.380
c	34	3+	1175.899830	1175.899636	-0.165
c	34	2+	1763.346107	1763.346490	0.217
c	35	3+	1214.576411	1214.576568	0.129
c	35	2+	1820.859579	1820.860110	0.292
c	36	3+	1247.924704	1247.924462	-0.194
c	20i	2+	1110.032142	1110.032427	0.256
c	21i	2+	1167.545613	1167.545686	0.063
c	34i	3+	1195.233316	1195.233951	0.531
y	3	1+	397.171777	397.171827	0.126
y	4	1+	484.203806	484.203771	-0.072
y	5	1+	541.225270	541.225281	0.020
y	6	1+	640.293684	640.293709	0.039
y	7	1+	754.336612	754.336563	-0.065
y	9	1+	942.416320	942.416353	0.035
y	10	1+	1029.448349	1029.448645	0.288
z	2	1+	266.126109	266.126109	0.000
z	3	1+	382.160877	382.160841	-0.094
z	4	1+	469.192905	469.192914	0.019
z	5	1+	526.214369	526.214338	-0.059
z	6	1+	625.282783	625.282678	-0.168
z	27	2+	1435.197489	1435.196299	-0.829
M+c	31	5+	1438.482615	1438.482645	0.021
M+c	32	5+	1458.496774	1458.496042	-0.502
M+c	32	4+	1822.618557	1822.618534	-0.013
M+c	33	5+	1469.700594	1469.699673	-0.627
M+c	33	4+	1837.375068	1837.375877	0.440
M+c	34	5+	1487.105911	1487.106523	0.412
M+c	34	4+	1858.883887	1858.883845	-0.023
M+c	35	6+	1258.761936	1258.761954	0.014
M+c	35	5+	1510.312868	1510.312981	0.075
M+c	35	4+	1887.891222	1887.891506	0.150
M+c	36	5+	1275.603219	1275.603316	0.076
M+c	36	5+	1530.924420	1530.924203	-0.142
M+c	34i	5+	1498.707009	1498.707619	0.407
M+c	34i	4+	1873.131943	1873.132905	0.514
M+z	2	3+	1391.654617	1391.655808	0.856
M+z	3	3+	1429.328685	1429.329444	0.531
M+z	4	3+	1458.339361	1458.340006	0.442
M+z	5	3+	1477.680667	1477.680895	0.154
M+z	6	3+	1510.369320	1510.368775	-0.361
M+z	7	3+	1548.049351	1548.049654	0.196
M+z	7	2+	2323.578098	2323.578660	0.242
M+z	8	3+	1582.400354	1582.401094	0.468
M+z	9	3+	1611.746974	1611.746700	-0.170
M+z	10	4+	1230.568102	1230.567991	-0.090
M+z	10	3+	1639.753258	1639.753036	-0.135
M+z	11	4+	1258.839125	1258.839593	0.372
M+z	11	3+	1677.447952	1677.447828	-0.074
M+z	12	4+	1287.110147	1287.110909	0.592
M+z	12	3+	1715.811104	1715.811618	0.300
M+z	13	4+	1304.869427	1304.869611	0.141
M+z	13	3+	1738.821678	1738.821082	-0.343
M+z	14	4+	1318.623443	1318.623189	-0.193
M+z	14	3+	1757.828832	1757.829081	0.142
M+z	14	2+	2638.247419	2638.246892	-0.200
M+z	15	4+	1355.390547	1355.390795	0.183
M+z	15	3+	1807.856058	1807.856380	0.178
M+z	16	4+	1384.147283	1384.147411	0.092
M+z	16	3+	1846.532522	1846.532903	0.206
M+z	16	2+	2769.295145	2769.294672	-0.171
M+z	17	4+	1412.904019	1412.903882	-0.097
M+z	17	3+	1884.874843	1884.874708	-0.072
M+z	18	4+	1434.912737	1434.912984	0.172
M+z	18	3+	1913.885523	1913.885178	-0.180
M+z	19	4+	1456.420033	1456.420238	0.141
M+z	19	3+	1942.896202	1942.895988	-0.110
M+z	20	4+	1491.186124	1491.186435	0.209
M+z	20	3+	1988.582507	1988.582942	0.219
M+z	21	4+	1515.953231	1515.953379	0.098
M+z	21	3+	2021.605320	2021.605553	0.115
M+z	22	4+	1544.224252	1544.224504	0.163
M+z	22	3+	2059.300020	2059.300910	0.432
M+z	23	4+	1580.489984	1580.489808	-0.111
M+z	23	3+	2108.322843	2108.323448	0.287
M+z	24	4+	1609.000716	1609.000938	0.138
M+z	24	3+	2146.337153	2146.337709	0.259
M+z	25	4+	1627.512008	1627.512645	0.391
M+z	25	3+	2170.350335	2170.351009	0.311
M+z	26	5+	1324.827880	1324.827646	-0.177
M+z	26	4+	1655.783015	1655.783415	0.232
M+z	26	3+	2208.046833	2208.046104	-0.330
M+z	27	5+	1356.048099	1356.048495	0.292
M+z	27	4+	1695.060261	1695.060550	0.170
M+z	27	3+	2260.080530	2260.081289	0.336
M+z	28	5+	1381.659815	1381.660250	0.315
M+z	28	4+	1726.824267	1726.823766	-0.290
M+z	29	5+	1402.069844	1402.069738	-0.076
M+z	29	4+	1752.086188	1752.086786	0.341
M+z	30	5+	1416.076777	1416.076531	-0.174
M+z	30	4+	1769.844153	1769.844536	0.216
M+z	34	5+	1491.103517	1491.103470	-0.032
M+z	34	4+	1864.130123	1864.130353	0.123
M+z	36	5+	1534.713228	1534.713224	-0.003
M+z	36	4+	1918.141132	1918.141912	0.407
M+z	16-i	4+	1370.399228	1370.399399	0.125
M+z	16-i	3+	1827.199153	1827.199447	0.161
M+z	17-i	4+	1399.406577	1399.406737	0.114
M+z	17-i	3+	1865.875642	1865.875456	-0.100

Average Error:	0.068
Absolute Average Error:	0.187
Standard Deviation:	0.245

Table S2. List of the assigned fragments from the ECD MS/MS spectrum of the 7+ charge state ((isoD)$_3$hIAPP) dimer ion. M represents one ((isoD)$_3$hIAPP) unit.
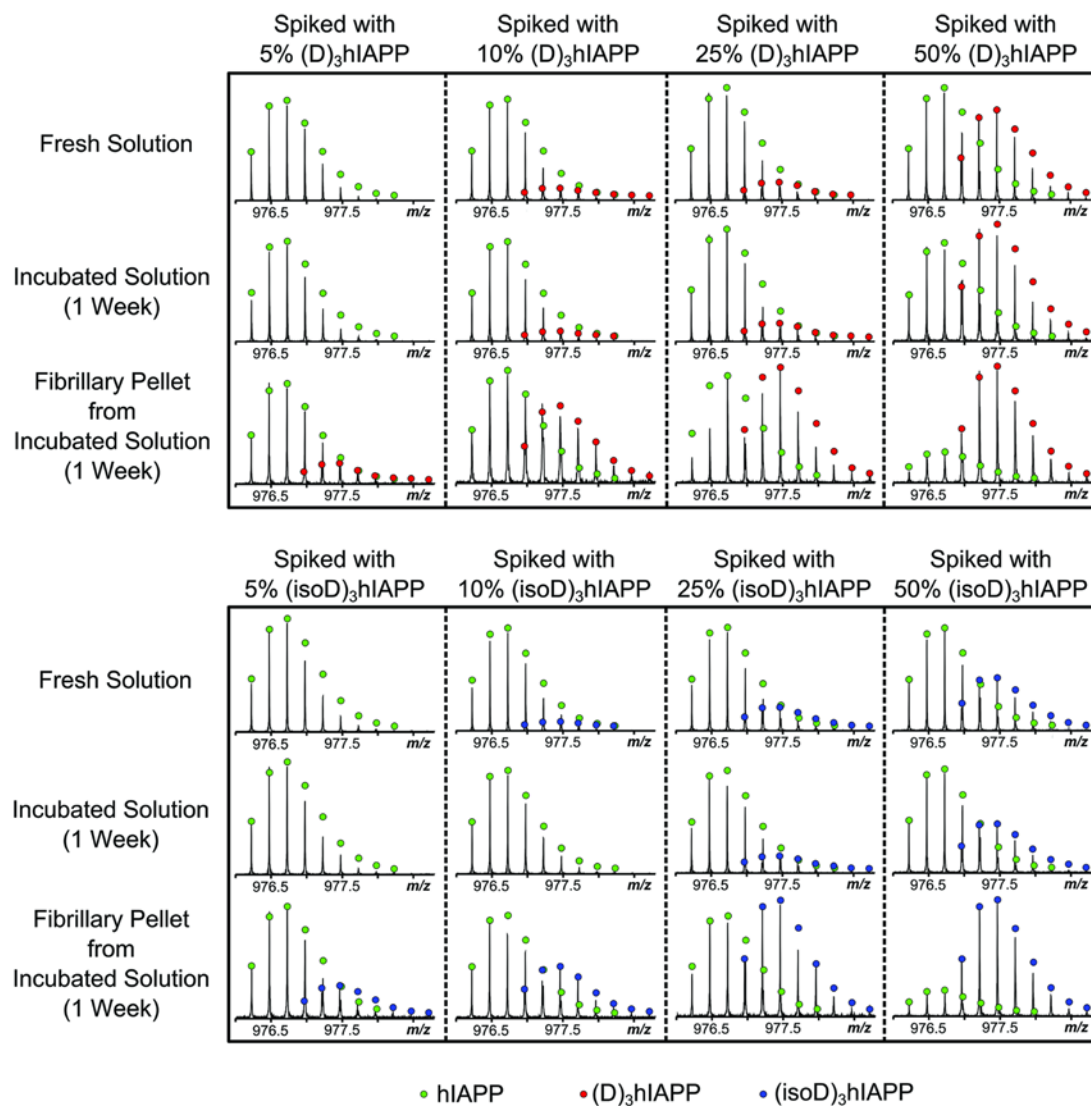
Figure S4. The nESI-MS spectra showing the fresh, the incubated solutions, and the incubated fibrillary pellets of hIAPP mixed with 5%, 10%, 25%, or 50% of mutant ((D)₃hIAPP) or ((isoD)₃hIAPP).